

Crystallization behavior of Si-added amorphous Ga₁₉Sb₈₁ films for phase-change memory

Po-Chin Chang^a, Chih-Chung Chang^a, Shih-Chin Chang^{a,*}, Tsung-Shune Chin^{b,**}

^a Department of Materials Science and Engineering, National Tsing Hua University, Hsinchu 30013, Taiwan, ROC

^b Department of Materials Science and Engineering, Feng Chia University, Taichung 40724, Taiwan, ROC

ARTICLE INFO

Article history:

Received 16 November 2012
Received in revised form 5 April 2013
Available online 24 May 2013

Keywords:

Si-addition;
Amorphous films;
Crystallization temperature;
Activation energy;
Johnson–Mehl–Avrami theory

ABSTRACT

Crystallization behavior of Si-added amorphous Ga₁₉Sb₈₁ films was studied by measuring electrical resistance (*R*) versus temperature (*T*) at various heating rates. The crystallization temperatures obtained from the *R*–*T* curves increase from 228 to 284 °C measured at the heating rate 10 °C/min with increasing Si content to 14 at.%. All films with full-crystallization show phases of Sb and GaSb. At 9 at.% Si the activation energy of crystallization and the rate factor reach the maxima of 9.1 eV and $6.8 \times 10^{84} \text{ min}^{-1}$, respectively. The kinetic exponent (*n*) of the film with 9 at.% Si is below 1.5 which indicates growth-dominated crystallization, while that of other films falls in $1.5 \leq n \leq 2.5$ which denotes decreasing nucleation rate during nuclei growth. Time of 90% crystallization slightly decreases owing to Si addition as estimated using JMA theory. The temperature corresponding to 10-year failure-time obtained through isothermal Arrhenius plot effectively increases from 156 to 217 °C as Si content is from 0 to 14 at.%. The melting temperature slightly reduces from 591 to 581 °C with Si addition. The reset voltage of test cells based on Si₄(Ga₁₉Sb₈₁)₉₆ is reduced by 0.5 V to ~2.75 V and can be set–reset switched within pulse-widths of 40–200 ns.

© 2013 Elsevier B.V. All rights reserved.

1. Introduction

There are tremendous demands on Flash memory for portable electronic devices such as digital camera, cellular phones and laptops [1]. Flash memory technology may encounter the physical limitations and uncertainties beyond 22 nm technology node [2]. Thus many emerging non-volatile memory technologies have been proposed such as phase-change RAM (PCRAM), resistive RAM (RRAM), and magnetic RAM [3]. PCRAM, switched based on reversible phase transition between amorphous and crystalline phases, has drawn much attention due to its high speed operation, long endurance, scalability, and cost-effectiveness [4,5].

Evolution of phase-change materials had been started since reversible phase transition of an amorphous semiconductor, Te–As–Si–Ge, was first observed by S. R. Ovshinsky in 1968 [6]. On the roadmap of developing phase-change materials, Ge₂Sb₂Te₅ (GST) is the most striking one because of its high crystallization speed, large resistance ratio between amorphous and crystalline states, long endurance and demonstrated feasibility [7–9]. However, GST has unsatisfactory properties like low crystallization temperature (*T_x*) hence unfavorable thermal stability and high melting temperature result appreciably to high reset current (*I_{res}*). As a consequence, doping elements

(N, O, Si, etc.) or dielectric materials (SiO₂, Ta₂O₅, HfO₂) in GST are usually manipulated to improve its phase-change properties [10–14].

Si-doped phase-change materials such as Si–Sb, Si–GeSb, Si–Sb₂Te, and Si–GST had been reported [11,15–17]. They all showed better thermal stability as compared with the pristine films. However, Si-doped Ga–Sb alloy has not been studied before. It has been proposed that Ga–Sb alloys show outstanding thermal stability and fast switching speed compared with GST [18,19]. Furthermore, the phase-change behavior of ultra-thin films had also been evaluated which paves the way to develop nano-scaled PCRAM devices [20]. In this paper, we endeavor to further improve the thermal stability of Ga–Sb alloys by doping Si. This is because Si can be easily incorporated into the films by either co-sputtering or ion-implantation methods [11,21]. One specific composition, Ga₁₉Sb₈₁, was chosen because of its growth-dominated crystallization behavior which could guarantee fast set operation [18]. The crystallization behavior, crystallized structure, thermal property and electrical switching of Si-doped Ga₁₉Sb₈₁ amorphous films were investigated in detail.

2. Experimental

Si-doped Ga₁₉Sb₈₁ films were deposited onto SiO_x/Si(100) substrates by radio-frequency magnetron sputtering method using three 2-inch targets GaSb, Sb, and Si, respectively. GST films were also prepared by using a stoichiometry target and studied for comparison. Film thickness was measured using an alpha-step (Veeco, Dektak 150 Stylus Profiler). The composition of 1000 nm films was analyzed by an

* Corresponding author. Tel.: +886 3 5715131x33847.

** Corresponding author. Tel.: +886 4 24517250x5323; fax: +886 3 5719868.

E-mail addresses: scchang@mx.nthu.edu.tw (S.-C. Chang), tschin@fcu.edu.tw (T.-S. Chin).

electron probe X-ray micro-analyzer (FE-EPMA, JEOL JXA-8500F). Electrical resistance (R) of 100 nm films at various ramping rates (10–50 °C/min) or holding temperatures, which were slightly below crystallization temperature, was measured using a two-probe method by a semiconductor analyzer (HP-4145B) in argon ambient. Crystal structure of films was inspected by a grazing-incident X-ray diffraction (GIXRD, Mac science MXP18) applying an incident angle 0.5° and a scanning rate 2°/min. Powered samples were obtained by scratching 1000 nm-films deposited on glass substrate of 15 cm in diameter. Thermal property of powdered samples was analyzed by a differential thermal analyzer (DTA, Perkin-Elmer, Diamond TG/DTA-6300). Test-cells of memory devices were fabricated by back-end-of-line CMOS process. The contact holes were with diameter of 600 nm. TiN was used as bottom electrode. The active layer of Si-added Ga₁₉Sb₈₁ being 50 nm in thickness and the top electrode TaN being 300 nm thick, were deposited consecutively onto the holes. Electrical performance of test-cells was conducted by a pulse-generator (Agilent 81110A) and a source-meter (Keithley 2400) to measure electrical resistance after set–reset switching.

3. Results

3.1. Composition, electrical resistivity (ρ) and crystallization temperature (T_x) of films

EPMA results of Si-doped Ga₁₉Sb₈₁ films were listed in Table 1. For simplicity, each composition was given a symbol based on Si content. For instance the Ga₁₉Sb₈₁ film with 9 at.% Si addition, the Si₉(Ga₁₉Sb₈₁)₉₁, is denoted as S9. Electrical resistance of 100 nm films with various Si contents as a function of temperature was measured at the heating rate 10 °C/min. The measured electrical resistance can be converted to electrical resistivity through the equation, $\rho = R \times d$, where d is the film thickness. The ρ - T curves are shown in Fig. 1. The T_x (°C) can be read from the minimal point of the first derivative of ρ - T curve. Resistivity at amorphous (ρ_a) and crystalline (ρ_c) states, resistivity ratio (ρ_a/ρ_c), and T_x are all listed in Table 1.

3.2. Structure analysis

Crystal structure of films at as-deposited and crystallized states was investigated by a GIXRD. Crystallized samples were taken from those after ρ - T measurements. The diffraction patterns of as-deposited and crystallized films are shown in Fig. 2(a) and (b), respectively.

3.3. Non-isothermal crystallization kinetics

The isothermal crystallization kinetics had been proposed by Johnson–Mehl–Avrami [22–25]. The transformation fraction (X) is expressed as the following equation,

$$X = 1 - \exp[-(Kt)^n]$$

Table 1

Composition, electrical resistivity at amorphous state (ρ_a) and crystalline state (ρ_c), resistivity ratio, and crystallization temperature (T_x) of Si-doped Ga₁₉Sb₈₁ films.

Power ratio (GaSb/Sb/Si)	Composition (at.%)	Symbol	Electrical resistivity ($\Omega \times \text{cm}$)		Crystallization temperature	
			ρ_a^a	$\rho_c (\times 10^{-4})^b$	ρ_a/ρ_c	T_x (°C) ^c
50 W/50 W/0 W	Ga ₁₉ Sb ₈₁	–	2.6	6.6	3.9×10^3	228
50 W/50 W/10 W	Si ₁ (Ga ₁₉ Sb ₈₁) ₉₉	S1	3.3	7.0	4.7×10^3	236
50 W/50 W/20 W	Si ₂ (Ga ₁₉ Sb ₈₁) ₉₈	S2	3.6	7.2	5.0×10^3	240
50 W/50 W/40 W	Si ₄ (Ga ₁₉ Sb ₈₁) ₉₆	S4	5.9	8.0	7.4×10^3	248
50 W/50 W/80 W	Si ₉ (Ga ₁₉ Sb ₈₁) ₉₁	S9	9.9	11.1	8.9×10^3	269
50 W/50 W/120 W	Si ₁₄ (Ga ₁₉ Sb ₈₁) ₈₆	S14	17.7	11.8	1.5×10^4	284

^a Resistivity measured at 30 °C.

^b Resistivity measured at 480 °C.

^c Deduced from R - T curve at heating rate 10 °C/min.

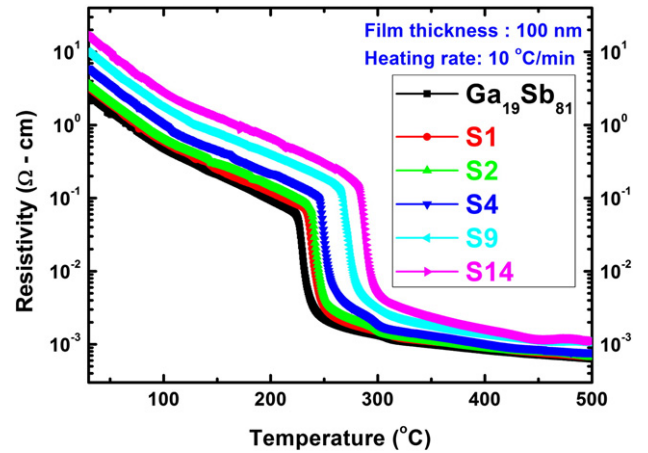


Fig. 1. Electrical resistivity (ρ) as a function of temperature (T) of Si-doped Ga₁₉Sb₈₁ films measured at the heating rate 10 °C/min.

where X is the transformation fraction, K (1/min) is the effective overall reaction rate, t (sec) is the time, and n is the kinetic exponent. K is usually expressed in the type of Arrhenius equation,

$$K = K_0 \exp\left(-\frac{E_a}{k_b T}\right)$$

where K_0 (1/min) is the rate factor, E_a (eV) is the activation energy, k_b (8.617×10^{-5} eV/K) is the Boltzmann constant, and T (K) is the temperature.

In fact, most experiments were conducted at a constant heating rate. As a result, several methods were developed to investigate crystallization kinetics under non-isothermal conditions such as Kissinger's method and Ozawa's method [26,27]. Rate factor (K_0) and activation energy of crystallization (E_a) can be derived from the Kissinger's plot. Kinetic exponent (n) can be deduced from the Ozawa's plot.

Film S1 was taken as an example for deducing kinetic parameters. Electrical resistance of films was measured at heating rates 10–50 °C/min as shown in Fig. 3(a). T_x can be deduced by differentiating resistance with temperature as shown in the inset of Fig. 3(b). The activation energy of crystallization (E_a) and rate factor (K_0) can be deduced by applying Kissinger's equation [26],

$$\ln\left(\frac{\alpha}{T_x^2}\right) = \ln\left(\frac{K_0 k_b}{E_a}\right) - \frac{E_a}{k_b T_x}$$

where α (°C/min) is the heating rate, T_x (K) is the crystallization temperature and k_b (8.617×10^{-5} eV/K) is the Boltzmann constant. Inset of Fig. 3(a) shows the Kissinger's plot. The values of E_a can be obtained from the slope of fitted line. K_0 can be calculated from the intercept of the fitted line to the y-axis. T_x , E_a and K_0 of all compositions including GST are all listed in Table 2.

Download English Version:

<https://daneshyari.com/en/article/7902773>

Download Persian Version:

<https://daneshyari.com/article/7902773>

[Daneshyari.com](https://daneshyari.com)